



Evaluation of thermal decomposition of Calcium Carbonate (CaCo₃) in the fault zone, a case study of the Astaneh fault

Mohammadreza Hajiannezhad, Behnam Rahimi *

Department of geology, Faculty of science, Ferdowsi University of Mashhad, Iran

Received: 22 October 2022, Revised: 22 February 2023, Accepted: 01 March 2023

© University of Tehran

Abstract

Astaneh fault is one of the active and seismic faults in the southern part of eastern Alborz. Performance of seismic faults in carbonate rocks and favorable conditions causes the change in Calcium Carbonate (CaCo₃) and its conversion to Calcium Oxide (CaO) or its thermal decomposition. If the environment is suitable for this deformation, after initial deformation, the primal volume is reduced, leaving the space available for depletion between deformed particles, which can be used as a key for this earthquake slip. During the Astaneh fault at the location where the fault occurred in the carbonates, after sampling the fault core and fault gouge, and photographing and studying them by SEM electron microscopy, the presence of Co₂ exit bubbles and the reduction of Calcium Carbonate (CaCo₃) volume caused by the earthquake slip heat created was observed at the nanoscale and micro level. After observing the thermal decomposition of Calcium Carbonate (CaCo₃) in the fault gouge, the reduced volume of particles was calculated from the earthquake slip heat. With the proportion between this volume reduction and the temperature causing it the temperature resulting from the seismic slip causing this deformation is estimated for the sampling location and fault surface.

Keywords: Astaneh Fault, Earthquake Slip, Thermal Decomposition Of Calcium Carbonate (Caco₃), Fault Gouge, Volume Reduction.

Introduction

The results of seismic slip function in faults can be seen in different ways. These include specific rocks from the slip (such as pseudotachylyte), deformation of minerals and rocks, and even the metamorphism of rocks due to the pressure and heat caused by Seismic slip, and so on. Conversion of Calcium Carbonate (CaCo₃) to Calcium Oxide (CaO) by heat and thermal decomposition of Calcium Carbonate as an endothermic phase before Calcium Carbonate metamorph in carbonate rocks and dehydration of clays can be considered as examples of the deformation of minerals due to heat. That can be checked in the fault rocks and can be considered as the result of frictional heat generated during seismic slip (Brantut et al., 2008; Sulem & Famin, 2009; Kuo et al., 2011). At ground level and atmospheric pressure, each of these changes occurs in a specific temperature range, which has been identified and introduced by various experiments and can be used as a key to detecting temperature changes during deformation (L'vov, 2002; Han et al., 2010; De paolo et al., 2011; Kohobhange et al., 2019).

Earthquakes play a key role in the evolution of architecture and fault structure. The structure of the fault zone and its related properties, such as permeability, anisotropy, lithology, etc. have significant control over fault evolution (Faulkner et al., 2010). The existence of many similarities between geology and seismology of faults shows that earthquakes play an

* Corresponding author e-mail: b-rahimi@um.ac.ir

undeniable role in the structural evolution of faults (Valoroso et al., 2014). What remains in nature for field and laboratory studies and available for study is the result of earthquake operations in a fault, which includes slipping of layers, structural and texture changes in rocks and minerals, macro, micro and nanostructures formed in rocks and mineral deposits, transformation and deformation, and the emergence of new rocks (fault rocks) and so on.

It should be noted that pseudotachylyte is one of the recognized fault rocks from an earthquake in a fault (McKenzie & Brune, 1972; Sibson, 1975; Di Toro et al., 2005a & b; Lin, 2008, 2019). Researchers are trying to find other rocks with different characteristics to understand the occurrence of earthquakes in a fault and consider some structural and textural properties of these rocks (Hirono et al., 2007; Boullier et al., 2009; Rowe et al., 2012; Smith et al., 2013; Laurich et al., 2014). The pseudotachylyte, of course, is a deep rock that will sharply deform if exposed (Sibson, 1975; Camacho et al., 1995; Di Toro et al., 2005a; Sibson & Toy, 2006; Lin, 2008). What will surely happen in the coseismic behavior of a fault is the increase in critical slip heat and pressure over a short period. Based on the depth and position of the faults and the thermodynamic properties of the earth, the result of this increase in pressure and heat is the change in the textural, structural and mineralogical shape of the rocks. Among the micro and nanostructures that result from frictional overheating in faults located in calcareous rocks is the thermal decomposition of Calcium Carbonate (CaCO_3) and also in areas with phyllosilicate minerals of dehydration clays (Brantut et al., 2008; Sulem & Famin, 2009; Han et al., 2010; Bullock et al., 2015; Kohobhange et al., 2019). Surely, by investigating these deformations in the future, more connections and communications between earthquake occurrences and their occurrence will be achieved.

In recent years, many studies have been conducted to investigate the textural and structural characteristics of fault rocks in the fault zone in different regions. Recently, many scientists have studied the micro and nanostructures in the fault rocks, which is an important field and can provide important evidence of how the coseismic slip occurs. This article is the result of the study of micro and nano structures in the fault gouge inside the carbonate rocks in a seismic fault (Astaneh). In this research, an attempt has been made to prove the thermal decomposition process of calcium carbonate based on evidence such as the presence of calcium oxide phase in the fault gouge. As a result, according to the characteristics and other conditions of this deformation, the heat that causes it, which is the result of seismic slip, can be obtained. It is worth noting that the results of this study will be a growing field in recent research.

The position and characteristics of the fault core in the active fault Astaneh

Astaneh's fault with the direction of the Northeast-Southwest is located in the western part of the sinistral Shahrood fault system. This fault is located in the southern part of Eastern Alborz, with a length of more than 95 km, and with Left-lateral strike-slip component is one of the major structures in this region (Rahimi, 2002; Jackson et al., 2002; Nazari, 2006; Nemati et al., 2012; Hollingworth et al., 2010; Rizza et al., 2011). Geologically, this fault is between the dolomitic deposits of the Jurassic limestone (Lar Formation) and the young alluvial deposit on the north side of the fault (hanging wall) against the shale and sandstones of the Jurassic and Triassic sandstone dolomite on the south side of the fault (foot wall) is located. In most of its length, this fault has at least two more or less parallel fault lines. These two branches of the fault with a distance of about 15 to 500 meters together with the sub-branches of the fault make a relatively large fault zone. Along it, a valley with a relatively flat floor has been formed with significant coverage of Quaternary deposits (Fig. 1. Tectonic map of Astaneh region).

The geomorphological evidence along the part of the fault that passes through the lithological units such as Shemshak, Dalichay and Lar formations indicates the uplift of the northern block and the subsidence of the southern block. And according to the slope of the fault surface, which is towards the north-west, it can be concluded that Pre-Quaternary movements of this fault have

shown a dominant reverse mechanism. Regarding the current mechanism of this fault based on the outcrops of the north and east of the village of Astaneh and also the existing sections in the Quaternary deposits, Marls, and the displacement of streams, its movement certainly can be sinistral. Although the rise of the northern block and its thrust on the south block is quite evident, the existence of completely horizontal and intact slickenside without weathering and erosion in two adjacent surfaces of this fault indicates that the last movement of this fault is Strike-slip and left lateral (Fig. 2 & 3).

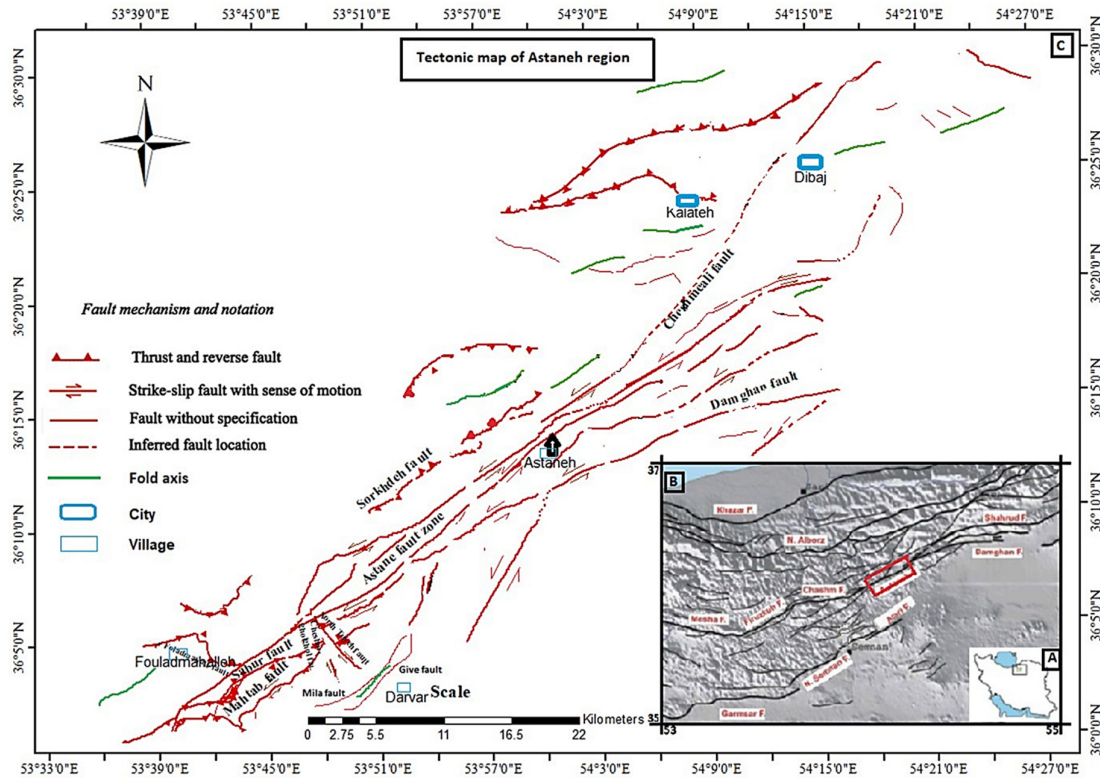


Figure 1. Tectonic map of the Astaneh and Indicative faults. A. Geographical location of Eastern Alborz in Iran, B. The location of the main faults of Eastern Alborz that the Astaneh area is located inside the red rectangle. and C. Tectonic map of the Astaneh and surrounding areas and the location of the faults in these areas. (The location of sampling and study is marked with a black dot)

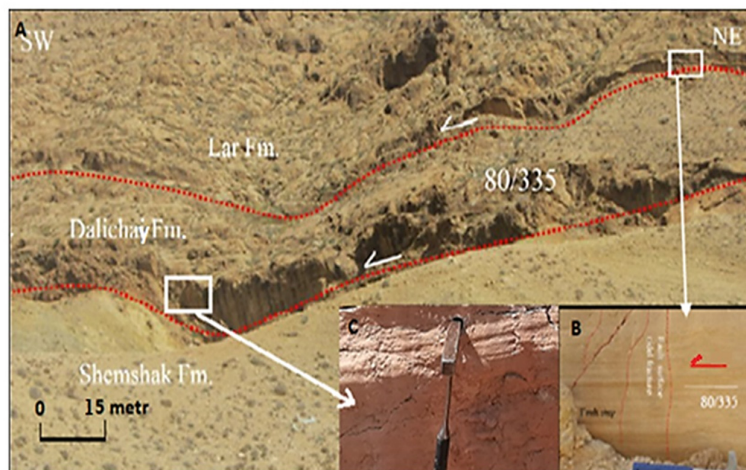


Figure 2. A. A view of two surfaces of the Astaneh fault, and B & C Horizontal slickensides associated with two fault surfaces north of Astaneh village

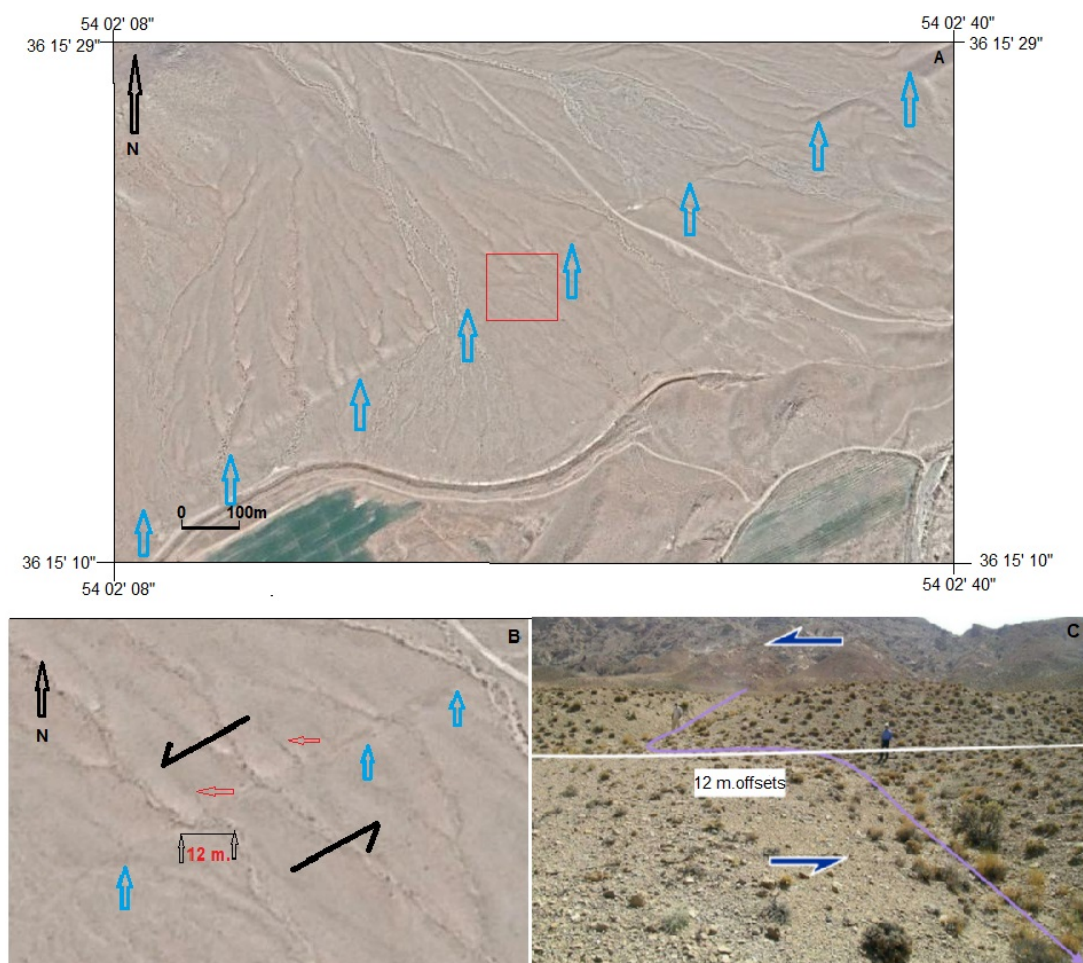


Figure 3. A. Google Earth image of the Astana fault in the east of Astaneh river. The blue arrows show fault trace on the ground in which the left lateral movement of the streams can be recognized .B. Enlarged form of the red rectangle in figure A. C. The view on the ground from the figure of A and B, where the movement of the stream is visible in a left-lateral direction

There is an intact and almost perfect fault zone in Astaneh village. There are two parallel fault surfaces, creating deep joints, fractures, and cracks along the perpendicular to large fractures. The operation of other large and small faults in the region caused by tectonic forces has created a faulting zone. This zone within the Cretaceous limestone (Lar Formation) has a transverse width of 500 meters, which consists of ample fault surfaces in parallel. Because of the heterogeneity of the lithology, the fault zone is an example of an anisotropic structure. With this explanation, along the length of the fault zone, there are differences from each other at different points both transversely and longitudinally.

In the Astaneh fault, in some regions, both the fault core and the damage zone can be observed. However, the fault gouge in the core of this fault is discrete and up to 35 cm thick in some areas. In fault core existence limestone (carbonate) fault gouge that maximum shear changes occurring. The mechanism of cataclastic rocks at the core of the fault is different during the length of the fault and in different locations and outcrops related to different times. Accordingly, to access the original fault gouge with a good diagonal and intact, after the field survey, the best region was detected in the north of Astaneh village. Then, after photographing by SEM, the images were analyzed and interpreted to perform the Calcium carbonate thermal decomposition process at the fault surface.

Methods

Faults fabric and earthquake slip are closely related to each other, which is referred to in many new papers. The most current and common way of understanding the events occurring in the seismic slip is to study the fabric and macro, micro, and nanostructures in the rock fault (Di Toro et al., 2006; Delle piane et al., 2017). Rock weakening processes such as increasing pore fluid pressure, frictional and rubbing melting, and thermal pressure include seismic slip events and are included in them. Some fault rocks created during a seismic slip retain evidence of physical and chemical properties during an earthquake (Scholz, 2002; Han et al., 2010; Ferraro et al., 2018; Ming et al., 2022). This type of rock can be referred to as pseudotachylyte, which is created by thermal activity during a seismic slip (Sibson, 1975; Cowan, 1999; Allen, 2005; Sibson & Toy, 2006; Di Toro et al., 2009; Rowe et al., 2012a; Smith et al., 2013).

Microstructures that formed during an earthquake are important for a better understanding of the earthquake (nucleation) and its progression process. Recently, high-speed friction experiments in carbonates and clays gouge have shown that the disintegration of minerals due to the heat of rubbing accelerates the thermal decomposition of calcite (Calcium carbonate) and dehydration of phyllosilicates results. The mechanism of these deformations can be grouped into four major categories, including breakdown processes, intra-crystalline deformation, recrystallization, and large mass distribution.

Of these four classes, the intra-crystal deformation should be considered as a microstructure that is micro and nanometer in size and occurs in crystal grains. This deformation is dependent on several mineralogical parameters including pressure, temperature, stress amount, strain rate, and pore fluid pressure. However, in a static recrystallization incident when the heat is externally applied or caused by a re-fabrication change, the deformation might occur.

Thermal decomposition in Calcium Carbonate (CaCO_3) starts from 700 to 750 degrees and continues to 950 degrees Celsius (Todor, 1976; L'vov, 2002; Alejandro et al., 2022). This decomposition in the fault zone is an indication of an increase in frictional heat during the earthquake. In the laboratory, high-speed friction experiments in the frictional heat resulting from slipping the layers up to 950 degrees in the earthquake is one of the reasons for the decarbonization of Calcium Carbonate (CaCO_3) and at lower temperatures up to 500 degrees, dehydration of the phyllosilicates (Faulkner et al., 2010; De Paolo et al., 2011; Kuo et al., 2011). Certainly, the decarbonization phase and the dehydration of microstructures can be used as a record of earthquake slip (Kuo, 2011; Collettini et al., 2013).

In the thermal decomposition process of Calcium Carbonate (CaCO_3) at 950 ° C, the maximum mass reduction occurs and the weight changes are fixed, indicating the completion of the reaction. However, with increasing particle size and heating rates, the reaction shifts to higher temperatures. As the heating rate increases, the sample is given less time to penetrate and react (L'vov et al., 2002; Nobari et al., 2006). This thermal decomposition results in the formation of Calcium Oxide (CaO) from Calcium Carbonate (CaCO_3) and the release of Carbon Dioxide (CO_2). This process plays a role in many geological processes known as Calcination. One of the places where this reaction occurs is in the limestone faults that happen due to the increase in temperature during seismic and coseismic slipping. (Smith et al., 2013; Collettini et al., 2013; Ünal-Imer et al., 2016; Delle Piane et al., 2017).

After field surveying, scrutiny, and studying the geological status, erosion, and weathering of the Astaneh fault surface along the fault, due to the presence of physically good structures on the fault plane as well as the function of the fault in calcareous lithology (Lar and Dalichay Formations), the area north of the Astaneh village was chosen for the study of tiny and microstructures. Among the most important reasons for choosing this area for more detailed investigation and study, the following can be mentioned: the presence of a pristine and unweathered fault surface, completely intact slickenside, limestone fault rocks with a thickness

of more than 3 meters in the core of the fault, and the presence of a fault gouge with varying thicknesses of 10 to 35 cm. Geographically, the study region is located between latitude of $36^{\circ} 16' 13.12''$ N- $36^{\circ} 16' 27.28''$ N and longitude of $054^{\circ} 05' 20.79''$ E- $054^{\circ} 05' 55.19''$ E.

In the next step, from different points, 6 cores were taken of the fault core perpendicular to the fault surface and 6 samples were taken from the fault gouge perpendicular to the gouge length. Due to the to be soft and not hardened of the gouge, samples were taken from buried gouges in the ground. Although it is recommended that the gouge samples be taken in this way due to the water absorption process and the change in the composition of the Calcium Oxide (CaO) on the surface of the earth. During the sampling operation, to avoid interference, different parts of the gouges were separated from each other (based on the distance from the fault surface). After this step, the thin sections from fault cores were prepared and polished, in which no particular cases were observed after studying under polarization microscopy (in this size).

Samples were then prepared and studied for SEM microscopy. At this stage, the best images of the fault troughs were obtained and in the magnification range of 12000 to 15000 the best photos were observed. The pores resulting from the activity of thermal decomposition can be seen as irregular shapes and cavities inside Calcium oxide (CaO). To avoid repetition of contents and images, only two typical photos of this process are included (Fig 4 A & B).

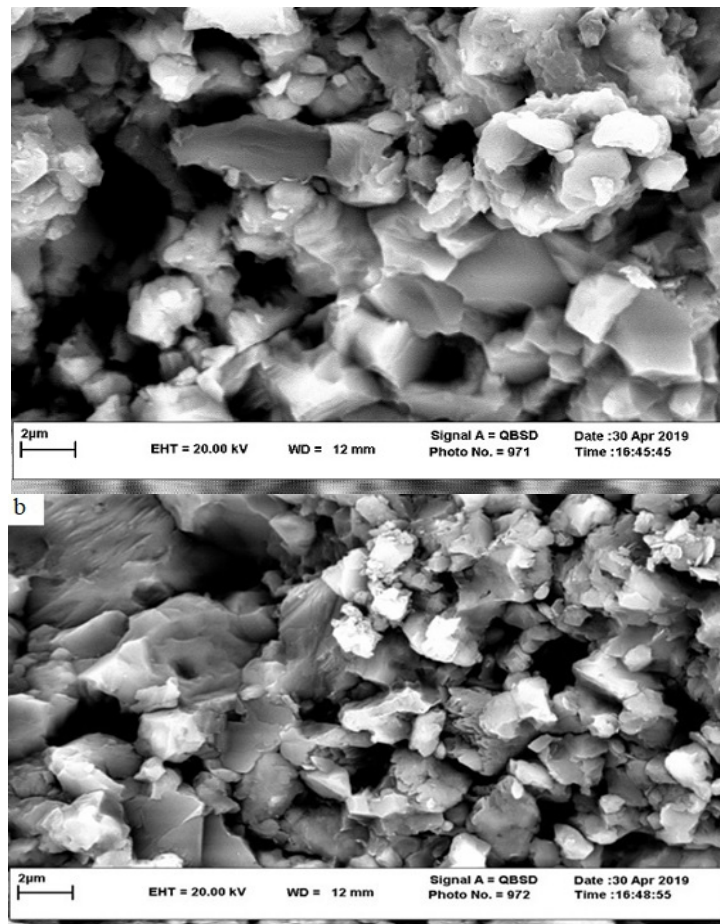


Figure 4. A. B. Two random photo samples of the Astaneh fault gouge taken on April 30th, 2019 by SEM microscope with a magnification of 15000 times in which white CaO are seen around the annular cavities. Dark areas indicate voids within the other particles. There is a white CaO around the voids caused by the thermal decomposition of Calcium Carbonate (CaCO_3). The area of the voids in Fig 6. was measured in three places. Note that the shape of the holes is irregular and their area and volume are proportional to the amount and percentage of thermal decomposition of Calcium Carbonate (CaCO_3)

It should be noted that some of these empty spaces (black in the photo) are not the result of thermal decomposition and are the result of the roughness of the sample surface. But many others that can be seen with a change in color at the fringes are the result of this activity which are circular in shape and white Calcium oxide (CaO) can be seen in their margins. Of course, it should be noted that each of these cavities is the result of changing the composition and reducing the volume of several grains together. In general, the process of changing the composition in each of the grains is done from the outside of the grains to the inside and center. (wiley, 1999; Stanmore et al., 2005; Collettini et al., 2013; Fig 4, 5 &6).

Discuss

The calcination process is influenced by three internal factors (particle size, impurities, and Carbon Dioxide vapor pressure) and external factors (heat rate, time, and the amount of heat), among which the particle size and heat play a more important role than the others (Stanmore et al., 2005). Based on the frictional heat generated by the slipping of the layers during the earthquake, the temperature increases, and the amount of this temperature increase depends on the slip rate and other mechanical properties. This heat in calcareous rocks is one of the reasons for the thermal decomposition of Calcium Carbonate (CaCO_3) and in temperatures below 500°C , dehydration of phyllosilicates. The process of calcination is an endothermic process, which can be illustrated as follows. (Todor, 1976; L'vov, 2002; Stanmore et al., 2005; Mohamed et al., 2012)

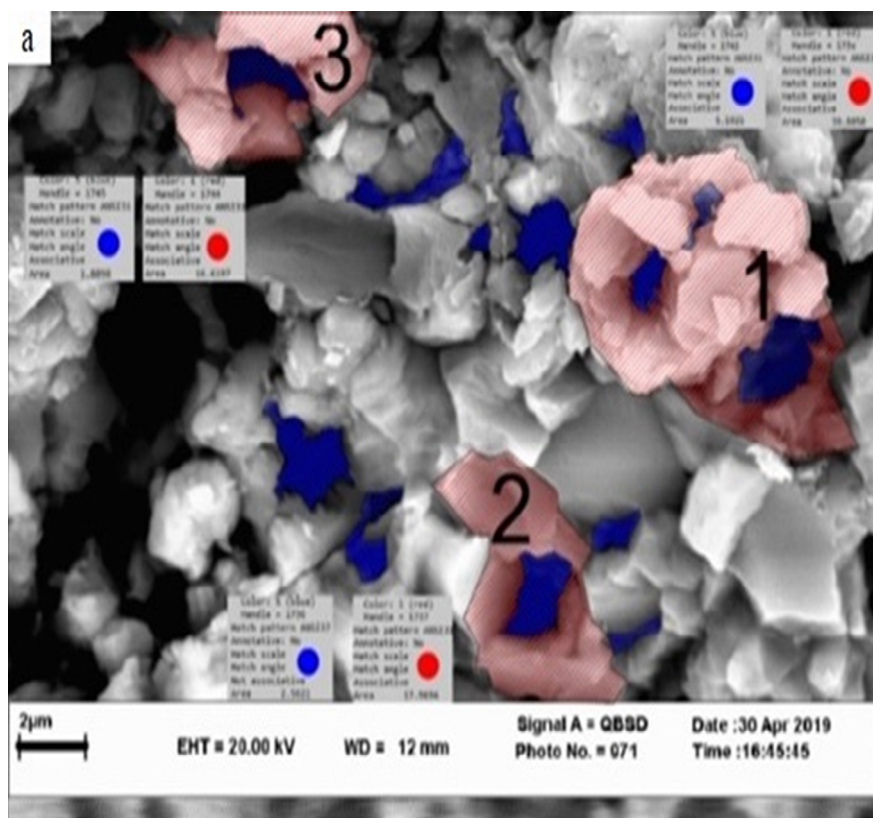


Figure 5. This is Figure 4 A, in which the free space area and thermal decomposition part are measured by AutoCAD in three parts. The blue part shows the free space and the red part shows the thermal decomposition area. In part 1, the area of the red part is $23.2301\ \mu\text{m}^2$ and the blue part is $3.7783\ \mu\text{m}^2$. In part 2, the area of red is $23.300\ \mu\text{m}^2$ and blue is $2.8700\ \mu\text{m}^2$. In part 3, the area of red is $20.7617\ \mu\text{m}^2$ and blue is $4.8319\ \mu\text{m}^2$. An example of determining the percentage of elements (EDS) for location number 1 is shown in Figure 7

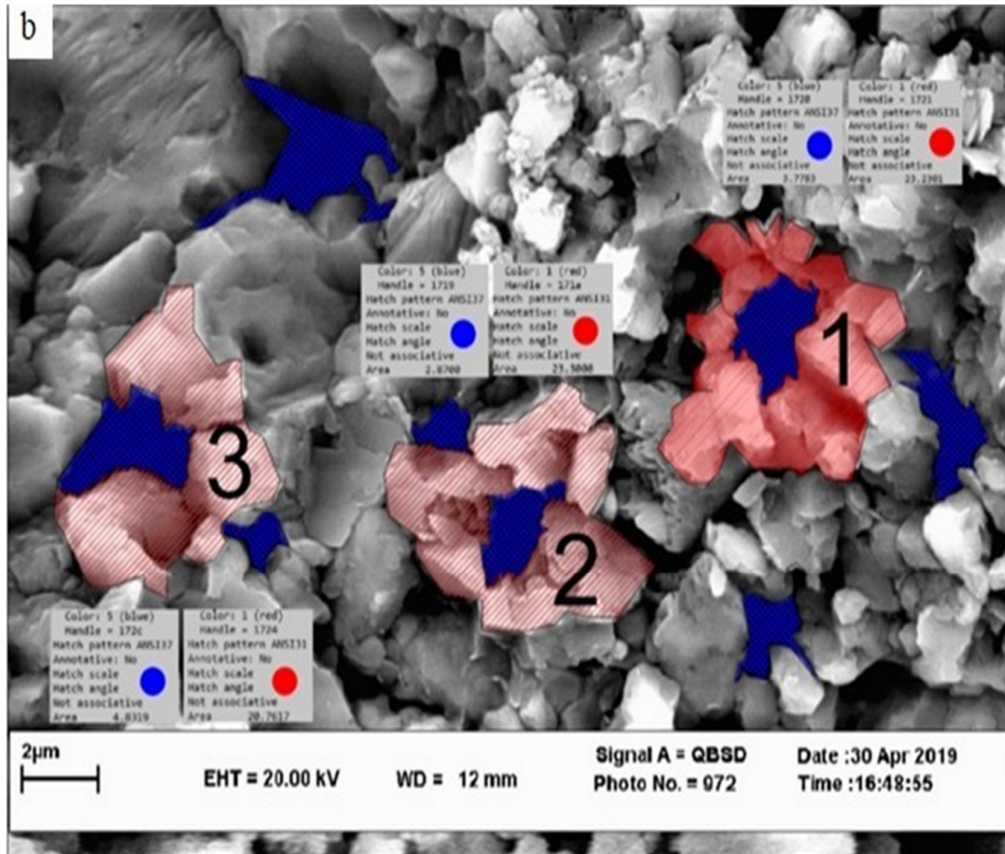


Figure 6. This is also figure 4b, where the free space and the thermal decomposition part have been measured by AutoCAD in three parts. The blue part shows the free space and the red part shows the thermal decomposition region. The red sections indicate the thermal decomposition of calcium carbonate (CaCO_3) or the sections of calcium oxide (CaO), and the blue sections show the reduction of the volume of calcium carbonate (CaCO_3) effective in thermal decomposition. In part 1, the area of the red part is $39.8050 \mu\text{m}^2$ and the blue part is $5.1921 \mu\text{m}^2$. In part 2, the area of red is $17.9694 \mu\text{m}^2$ and blue is $2.5621 \mu\text{m}^2$. In part 3, the area of red is $16.6197 \mu\text{m}^2$ and blue is $1.88 \mu\text{m}^2$



In the production of the fault gouge, both the increase in friction temperature and decrease the particle size which is much smaller than 2 mm, are effective in the deformation. According to the shrinking core model, Calcium Carbonate (CaCO_3) transformation to Calcium Oxide (CaO) starts from the outer layer of the particle and progresses inward until the entire crystal and crystal particle are decomposed (Wiley, 1999). All reactions in the laboratory occur with an increase in temperature in the range of 750 to 950 ° C with a major reduction in Calcium Carbonate (CaCO_3) weight due to the decomposition reaction and Carbon Dioxide emissions and at temperatures above 950 ° C, the weight remains unchanged which confirms the completion of the reaction. These experiments show that by increasing the particle size and the heating rate, the reaction shifts to higher temperatures. In all these experiments, the weight loss of the sample indicates the fraction of the sample that decomposes during the reaction (sanders et al., 2002). The higher the heating rate, the lower the reaction rate because with the increase in the heating rate, less time is given to the sample to penetrate and perform the reaction. And the smaller the particle size, the higher the decomposition rate. However, Chonge (2006) believes that as the sample size increases, the effective surface area of the sample increases, which distributes more efficient heat transfer. This factor speeds up the process by reducing thermal resistance and other resistances such as mass transfer or gas distribution. At higher

heating rates, the temperature difference between the surface and the core of the grain and mineral is greater, and therefore the time required to achieve equilibrium will be longer because the surface of the particles will be heated first and then it will be heated through the penetration of the core of the sample.

Based on the results of XRD and DTA/TGA in the tested samples, Calcium Carbonate (CaCO_3) decomposition occurs in the temperature range of 750 to 950 degrees Celsius. The Thermo-gravimetric results showed that the sample decomposition starts at a temperature of about 750 degrees Celsius. This reaction ends with a change in composition and about 44% weight loss at a temperature of 950 degrees Celsius. Samples with smaller particles show a higher decomposition rate in a shorter time and lower temperature compared to other samples. It also indicates that the Calcium Carbonate (CaCO_3) decomposition rate and time go up as the heating rate increases (Lvov et al., 2002; Mohamed et al., 2012; Chong et al., 2006; Collettini et al., 2013; Hurst, 1991).

Investigation and Analysis of the Thermal Decomposition Process in Calcium Carbonate (CaCO_3) in the Astaneh Fault

After SEM shooting and checking the photos, the area of different parts deformed by thermal decomposition and the empty space resulting from this process was measured by AutoCAD software, which is shown in Fig. 5.&6. It should be noted that the selected images are mostly based on the appearance of the samples and the samples were randomly selected for study and there were no specific instructions for selecting the images. Accordingly, in the two pictures, for each of the three marked sections showing the transformation of Calcium Carbonate (CaCO_3) to Calcium Oxide (CaO), the area was measured. It should be noted that it is not possible to produce a 3D image of this size of samples by SEM. And for this reason, we have to calculate and measure the reduced surface due to thermal decomposition and measured it in different places and different images. And because the samples were prepared for imaging from different directions and different angles and systematically from the thickness of the gouge, surely the area measured in the samples will have a direct relationship and natural proportion with the corresponding volume. Therefore, the area reduction in each of the marked parts is based on percentages as follows.

The area of the created hole (empty space) /area of calcium oxide around it*100 = Percentage of surface reduction

In the first photo (Fig 4A & 5):

- 1) $5.1921 \mu\text{m}^2 / 39.8050 \mu\text{m}^2 = 0.1304383871372943 * 100 = 13.04 \%$
- 2) $2.5621 \mu\text{m}^2 / 17.9694 \mu\text{m}^2 = 0.1425812770598907 * 100 = 14.26\%$
- 3) $1.8898 \mu\text{m}^2 / 16.6197 \mu\text{m}^2 = 0.1137084303567453 * 100 = 11.37 \%$

In the second photo (Fig 4 B. and 6.):

- 1) $3.7786 \mu\text{m}^2 / 23.2301 \mu\text{m}^2 = 0.1626467384987581 * 100 = 16.26\%$
- 2) $2.8700 \mu\text{m}^2 / 23.3000 \mu\text{m}^2 = 0.1231759656652361 * 100 = 12.32 \%$
- 3) $4.8319 \mu\text{m}^2 / 20.7617 \mu\text{m}^2 = 0.2327314237273441 * 100 = 23.27\%$

In general, the average volume reduction in images for the calculated locations is as follows:

In the first photo (Fig 4 A & 5): $(13.04 \% + 14.26\% + 11.37\%) / 3 = 12.89\%$:

And in the second photo (Fig 4 B & 6): $(16.26 \% + 12.32\% + 23.27\%) / 3 = 17.28\%$

Therefore, the sample volume reduction in the first image is 12.89% and in the second is 17.28%. The maximum volume reduction by heat in Calcium Carbonate (CaCO_3) is 44% at 950 ° C. and there is no deformation and volume loss at 750 degrees. Thus at 200 degrees heat, we have a 44 percent volume reduction. And it is possible to calculate the minimum temperature that causes deformation with a ratio. It can be stated that in the first sample from which the

image was prepared the minimum temperature is 836 ° C. and in the second is 814.5 °C. Since the time of a seismic slip is up to a few several minutes and the samples are taken from the surface, according to the effective temperature in the Calcium Carbonate (CaCO_3) analysis, the slip temperature should be higher than this value. In any case, the thermal decomposition of Calcium Carbonate (CaCO_3) and its volume reduction in the Astaneh fault should be considered as a record of the seismic slip in the fault with a minimum slip temperature of 792 ° C., and a maximum of 840 °C. Table 1 shows the calculated thermal decomposition data of Calcium Carbonate (CaCO_3) in other images and examples. Here, in order to avoid the length of the text, it is sufficient to mention only the results.

It should be noted that due to the high similarity of energy dispersive spectroscopy (EDX) of calcium carbonate and calcium oxide in SEM images, it is difficult to prove the existence of each of these two phases (Fig.7). With this explanation, in order to definitively prove the calcium oxide phase, XRD analysis was necessarily performed on the SEM samples. Here, the result of the XRD test whose sample was prepared simultaneously and together with and adjacent to the samples related to SEM images, is presented to prove the presence of calcium oxide composition in the fault gouge (Fig. 8).

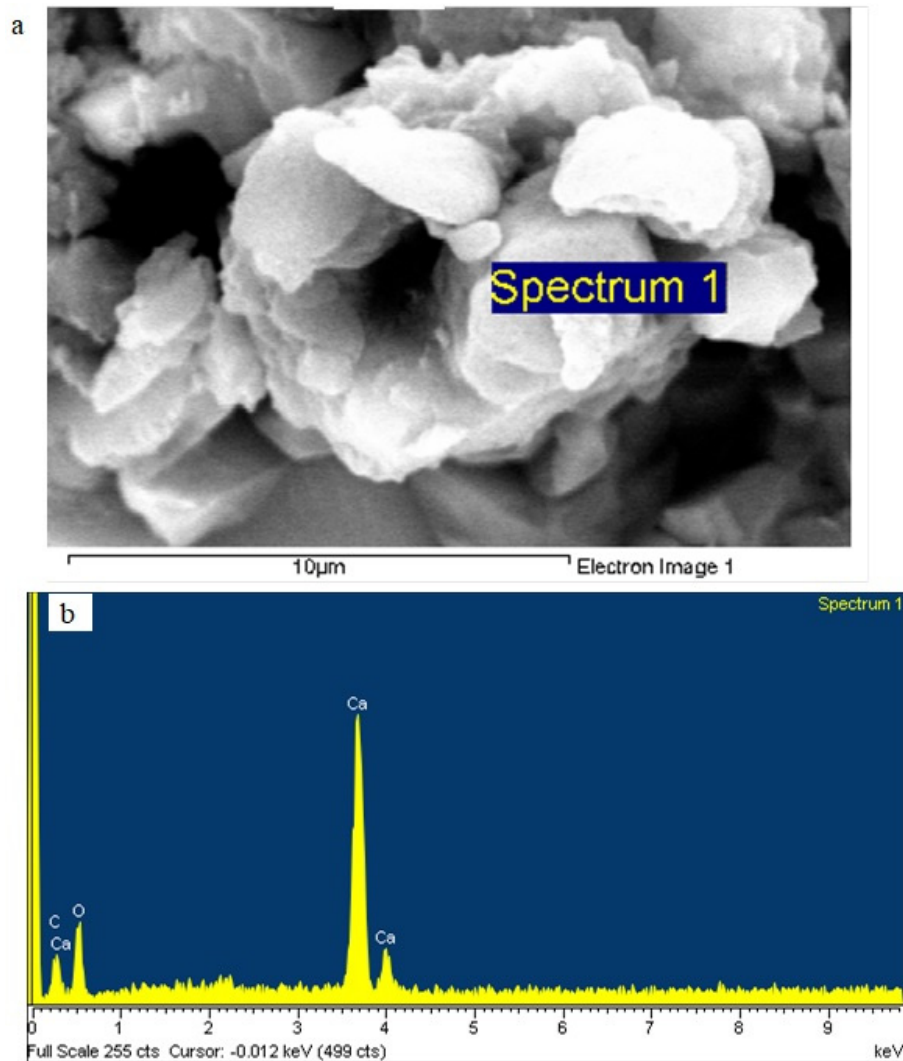
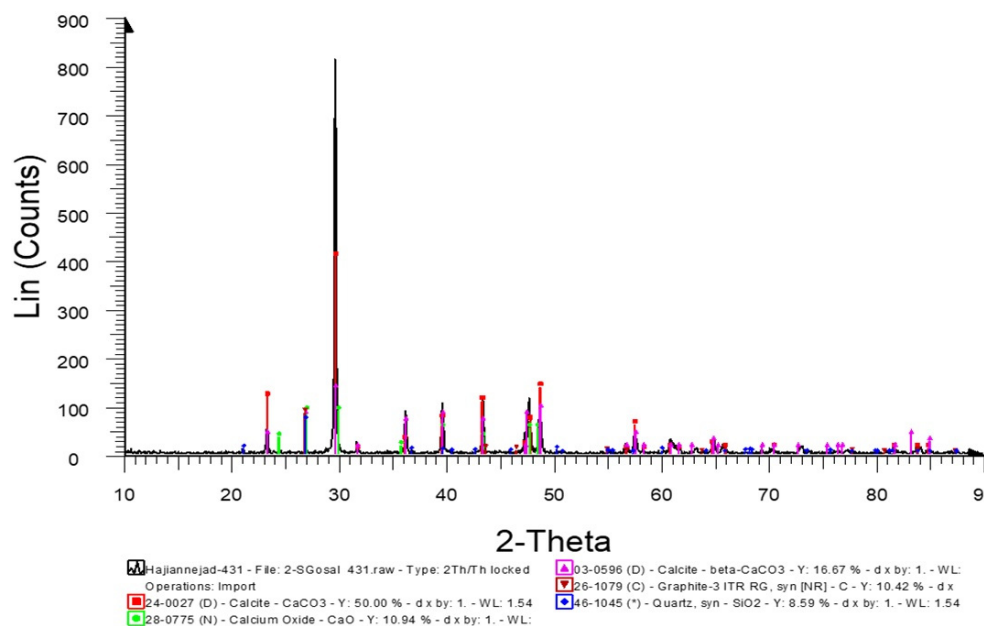


Figure 7. A. SEM figure and corresponding EDX diagram below for selected part of photos 4 A and 5.B. figure of EDX diagram of the selected part in figure a where Ca and O are two elements that show the composition of CaO from calcium carbonate (CaCO_3) in the fault gouge

Table 1. Results from other Calcium Carbonate (CaCo₃) thermal decomposition data in Astaneh fault gouge

Number	Decreased volume (Measured)	Deformed volume (Measured)	Volume reduction percentage (Calculated)	Deformation temperature (Calculated)
1	3.21 μm^2	26.410 μm^2	12.15%	811° C
2	2.12 μm^2	22.101 μm^2	9.6%	798° C
3	2.28 μm^2	27.121 μm^2	8.4%	792° C
4	3.41 μm^2	21.120 μm^2	16.15%	831° C
5	2.72 μm^2	22.200 μm^2	12.25%	811° C
6	2.92 μm^2	26.80 μm^2	10.9%	804.5° C
7	3.83 μm^2	21.130 μm^2	18.12%	840.5° C
8	3.62 μm^2	24.200 μm^2	14.95%	825° C

**Figure 8.** The diagram obtained from the XRD analysis belongs to the sample taken from gouge of Astaneh fault, in which the calcium oxide phase is 10.94%

Conclusion

Certainly, there are signs and traces of seismic slip in seismic faults, some of which are deformed over time and disappear as they outcrop the soil. Examples include rocks such as the pseudotachylyte. Apart from macro cases, micro and nano factors and signs can also be looked for in these faults to prove that they are seismic. Thermal decomposition of Calcium Carbonate (CaCo₃) and dehydration of clays should be classified into micro and nano categories in terms of size. If these things are present in the rock faults and fault surfaces, they are definitely the result of material change and deformation due to heat and pressure caused by seismic slip. These cases can be considered as seismic slip records. However, they should be searched for in faults with an intact fault zone that has not been altered.

Astaneh fault in the Southern domain of Eastern Alborz is an active and seismic fault that is associated with many systematic and historical earthquakes. This topic has been mentioned in different articles by different researchers (Hollingsworth et al., 2010; Nemati et al., 2012; etc.). In this fault due to the presence of a completely pristine and intact fault zone within the Delichay and Lar limestons, the presence of thermal decomposition of Calcium Carbonate (CaCo₃) might

refer to a seismic record.

Micro and nanostructure studies of fault gouges indicate that:

1. No nano and micro alignment and impression orientation can be seen in the gouge grains of the fault. For this reason, these grains have only endured compression, crushing, resizing, and deformation.
2. The thermal decomposition of Calcium Carbonate (CaCO_3) into Calcium Oxide (CaO) begins at the outer boundary of the grains and progresses inward, indicating that this change occurs simultaneously with crushing.
3. The Calcium Oxide (CaO) formed within the gouges is caused by the Calcium Carbonate (CaCO_3) decomposition after the gouge formation. As the gaps between the gouge particles did not remain the same and were not filled, there has been at least some time between the fault slipping and the crushing of minerals, rocks, and the resulting heat transfer.
4. Depending on the amount of space between the Calcium Carbonate (CaCO_3)-deformed particles, the deformation temperature should be around 740 to 816 degrees Celsius. This can certainly be increased at depths, and it is more likely to be checked if data from depths such as gouges and so on could be obtained.

Acknowledgements

This study was conducted as a part of the Ph.D. thesis of the first author (M. H.) at the Ferdowsi University of Mashhad (grant number: 3/44492). We thank the editor and two anonymous reviewers for their constructive and detailed reviews, which helped us to improve the paper considerably.

References

- Alejandro, J., Vicente R., Miguel A. V., 2022. Thermal study of the hydrocalumite-katoite-Calcium Carbonate (CaCO_3) system. *Journal of Thermochemica Acta*, 713 (2022) 179242.
- Allen, J.L., 2005. A multi-kilometer pseudotachylite system as an exhumed record of earthquake rupture geometry at hypocentral depth (Colorado, USA). *Journal of Tectonophysics*, 402: 37-54.
- Boullier, A-M., Yeh, E-C., Boutareaud, S., Song, S-R., Tsai, C-H., 2009. Microscale anatomy of the 1999 Chi-Chi earthquake fault zone. *Journal of Geochemistry Geophysics Geosystems*, 10(3): 1-25.
- Brantut, N., Schubnel, A., Rouzaud, J-N., Brunet, F., Shimamoto, T., 2008. High-velocity frictional properties of a clay-bearing fault gouge and implications for earthquake mechanics. *Journal of Geophysical Research: Solid Earth*, 11: 1-18.
- Bullock, R.J., De Paola, N., Holdsworth, R.E., 2015. An experimental investigation into the role of phyllosilicate content on earthquake propagation during seismic slip in carbonate faults. *Journal of Geophysical Research: Solid Earth*, 120: 3187-3207.
- Camacho, A., Vernon, R.H., Fitz Gerald, J.D., 1995. Large volumes of anhydrous pseudotachylite in the Woodroffe Thrust, eastern Musgrave Ranges, Australia. *Journal of Structural Geology*, 17: 371-38.
- Chong, C., Specht, E., 2006. Reaction rate coefficients in decomposition of lumpy Calcium Oxide (CaO) stone of different origin. *Journal of Thermochemica Acta*, 449: 8-15.
- Collettini, C., Viti, C., Tessei, T., Mollo, S., 2013. Thermal decomposition along natural faults during earthquakes. *Journal of Geology*, 41(8): 927-930.
- Cowan, D.S., 1999. Do faults preserve a record of seismic slip? A field geologist's opinion. *Journal of Structural Geology*, 21: 995-1001.
- Delle piane, C., Clennell, M., Keller, J., Giwelli, A., Luzin, V., 2017. Carbonate hosted fault rocks: A review of structural and microstructural characteristics with implications for seismicity in the upper crust. *Journal of Structural Geology*, 103: 17-36.
- De Paola, N., Hirose, T., Mitchell, T., Di Toro, G., Viti, C., Shimamoto, T., 2011. Fault lubrication and earthquake propagation in thermally unstable rocks. *Journal of Geology*, 39: 25-38.

- Di Toro, G., Pennacchioni, G., Teza, G., 2005a. Can pseudotachylytes be used to infer earthquake source parameters? An example of limitations in the study of exhumed faults. *Journal of Tectonophysics*, 402: 3-2.
- Di Toro, G., Pennacchioni, G., 2005b. Fault plane processes and mesoscopic structure of a strong-type seismogenic fault in tonalites (Adamello batholith, Southern Alps). *Journal of Tectonophysics*, 402: 55-80.
- Di Toro, G., Takehiro, H., Stefan, N., Giorgio, P., Toshihiko, S., 2006. Natural and Experimental Evidence of Melt Lubrication of Faults During Earthquakes. *Journal of Science*, 311: 647-649.
- Di Toro, G., Pennacchioni, G., Nielsen, S., Eiichi, F., 2009. Pseudotachylytes and earthquake source mechanics, in *Fault-zone Properties and Earthquake Rupture Dynamics*. *Journal of International Geophysics*, 94: 87-133.
- Faulkner, D.R., Jackson, C.A.L., Lunn, R.J., Schlische, R.W., Shipton, Z.K., Wibberley, C.A.J., Withjack, M.O, 2010. A review of recent developments concerning the structure, mechanics and fluid flow properties of fault zones. *Journal of Structural Geology*, 32: 1557-1575.
- Ferraro, F., Stefano Grieco, D., Agosta, F., Prosser, G., 2018. Space-time evolution of cataclasis in carbonate fault zones. *Journal of Structural Geology*, 110: 45-64.
- Han, R., Hirose, T., Shimamoto, T., 2010. Strong velocity weakening and powder lubrication of simulated carbonate faults at seismic slip rates. *Journal of Geophysical Research*, 115: 1-23.
- Hirono, T., Yokoyama, T., Hamada, Y., Tanikawa, W., Mishima, T., Ikehara, M., Famin, V., Tanimizu, M., Lin, W., Soh, W., Song, S., 2007. A chemical kinetic approach to estimate dynamic shear stress during the 1999 Taiwan Chi-Chi earthquake. *Journal of Geophysical Research Letters*, 34: 1-6.
- Hollingsworth, J., Nazari, H., Ritz, J. F., Salamati, R., Talebian, M., Bahroudi, A., Walker, R.T., Rizza, M., Jackson, J., 2010. Active tectonics of the east Alborz mountains, NE Iran: Rupture of the left lateral Astaneh fault system during the great 856 A.D. Qumis earthquake. *Journal of Geophysical Research*, 115: 1-19.
- Hurst, H.J., 1991. The thermal decomposition of magnesite in nitrogen. *Journal of Thermochemica Acta*, 189: 91-96.
- Jackson, J., Priestly, K., Allen, M., Berberian, M., 2002. Active tectonics of the South Caspian Basin. *Journal of Geophysical Journal International*, 148: 214-245.
- Janssen, C., Wirth, R., Lin, A., Dresen, G., 2013. TEM microstructural analysis in a fault gouge sample of the Nojima Fault Zone, Japan. *Journal of Tectonophysics*, 583: 101-104.
- Kohobhange, S.P., Karunadasa, H., Manoratne, H.M., Pitawala, T.G.A., Rajapakse, R.M.G., 2019. Thermal decomposition of Calcium Carbonate (CaCO₃) (Calcium Carbonate (CaCO₃) polymorph) as examined by in-situ high-temperature X-ray powder diffraction. *Journal of Physics and Chemistry of Solids*, 134: 21-28.
- Kuo, L-W., Song, S-R., Huang, L., Yeh, E-C., and Chen, H-F., 2011. Temperature estimates of coseismic heating in clay-rich fault gouges, the Chelungpu fault zones, Taiwan. *Journal of Tectonophysics*, 502: 315-327.
- Laurich, B., Urai, J.L., Desbois, G., Vollmer, C., and Nussbaum, C., 2014. Microstructural evolution of an incipient fault zone in Opalinus Clay: Insights from an optical and electron microscopic study of ion-beam polished samples from the Main Fault in the Mt-Terri Underground Research Laboratory. *Journal of Structural Geology*, 67: 107-128.
- Lin, A., 2008. *Fossil Earthquakes: The Formation and Preservation of Pseudotachylytes*. Springer-Verlag Berlin, Heidelberg, New York: Springer, 348 pages.
- Lin, A., 2019. Thermal pressurization and fluidization of pulverized cataclastic rocks formed in seismogenic fault zones. *Journal of Structural Geology*, 125: 278-284.
- L'vov, B.L., 2002. Mechanism and kinetics of thermal decomposition of carbonates. *Journal of Thermochemica Acta*, 386: 1- 16.
- McKenzie, D., Brune, J.N., 1972. Melting on Fault Planes During Large Earthquakes. *Journal of Geophysical Journal of the Royal Astronomical Society*, 29: 65-78.
- Ming, Z., Long, Y., Weichao, L., Zhengbo, W., Chenyang, Z., Qian, C., Bo, W., 2022. Frictional properties of the rupture surface of a carbonate rock avalanche. *International Journal of Rock Mechanics and Mining Sciences Volume*, 153:105088.
- Mohamed, M., Yusup, S., Maitra, S., 2012. Decomposition study of Calcium Carbonate (CaCO₃) in the cockle shell. *Journal of Engineering Science and Technology*, 7: 1-10.

- Nazari, H., 2006. Analyse de la tectonique récente et active dans l'Alborz Central et la région de Téhéran: Approche morphotectonique et paleoseismologique. Science de la terre et de l'eau. Ph.D. thesis. University of Montpellier2, pp: 247 (in France).
- Nemati, M., Hatzfeld, D., Gheitanchi, M.R., Sadidkhouy, A., Mirzaei, N., and Moradi, A., 2012. Investigation of seismicity of the Astaneh Fault in the East Alborz. *Journal of Earth and Space Physics*, 37(2): 1-16.
- Nobari, A.H., Halali, M., 2006. An investigation on the calcination kinetics of zinc carbonate hydroxide and Calsimin zinc carbonate concentrate. *Chemical Engineering Journal*, 121(2-3): 79-84.
- Rahimi, B., 2002. Structural Study of Alborz Range in North Damghan, Ph.D. thesis. University of the shahid Beheshti, Iran, pp.232 (in Persian).
- Rizza, M., Mahan, S., Ritz, J-F., Nazari, H., Hollingsworth, J., Salamati, R., 2011. Using luminescence dating of coarse matrix material to estimate the slip rate of the Astaneh fault, Iran. *Quaternary Geochronology*, 6:390-406.
- Rowe, C.D., Fagereng, A., Miller, J.A., Mapani, B., 2012. Signature of coseismic decarbonation in dolomitic fault rocks of the Naukluft Thrust, Namibia. *Earth and Planetary Science Letters*, 333-334: 200-210.
- Scholz, C. H., 2002. *The Mechanics of Earthquakes and Faulting*, Cambridge University. Cambridge University Press, pp: 471.
- Sibson, R.H., 1975. Generation of pseudotachylyte by ancient seismic faulting, *Geophysical. Journal of the Royal Astronomical Society*, 43: 775-794.
- Sibson, R.H., Toy, V.G., 2006. The habitat of fault-generated pseudotachylyte: Presence vs. absence of friction-melt. Published Online: 18 March 2013 Published Print: 01 January 2006. AGU (American Geophysical Union) Monograph, 170: 153-166.
- Smith, S.A.F., Di Toro, G., Kim, S., Ree, J-H., Nielsen, S., Billi, A., Spiess, R., 2013. Coseismic recrystallization during shallow earthquake slip. *Journal of Geology*, 41: 63-66.
- Stanmore, B.R., Gilot, p., 2005. Review: Calcination and carbonation of Calcium Oxide (CaO)stone during thermal cycling for CO₂ sequestration. *Journal of Fuel Processing Technology*, 86: 1707-1743.
- Sulem, J., Famin, V., 2009. Thermal decomposition of carbonates in fault zones: slip weakening and temperature-limiting effects. *Journal of Geophysical Research: Solid Earth*, 114: 1-14.
- Todor, D. N., 1976. *Thermal Analysis of Minerals*. Abacus Press, Published online by Cambridge University Press 2018 , 256 pp.
- Ünal-Imer, E., Uysal, I.T., Zhao, J-X., Is ik, V., Shulmeister, J., Imer, A., Feng, Y-X, 2016. CO₂ outburst events in relation to seismicity: constraints from microscale geochronology, geochemistry of late Quaternary vein carbonates, SW Turkey. *Journal of Geochimica et Cosmochimica Acta*, 187: 21-40.
- Valoroso, L., Chiaraluce, L., Collettin, C., 2014. Earthquakes and fault zone structure. *Journal of Geology*, 42(4): 1-5.
- Wiley, J., 1999. *Chemical reaction engineering*. (3rd Ed.), Levenspiel New York.



This article is an open-access article distributed under the terms and conditions of the Creative Commons Attribution (CC-BY) license.